XLIII CILAMCE
21–25, November, 2022
FOZ DO IGUAÇU – PR – BRAZIL

Computational method for estimating the emissivity of human skin under different conditions: dry skin, sweaty and with lotion

João T. Lemos[1], Andriele Ninke[2], Josemar Simão[2], Hércules L. M. Campos[3], Reginaldo B. Nunes[1], Pablo R. Muniz[1]

[1]*Postgraduate Program in Sustainable Technologies, Federal Institute of Espírito Santo*
Av. Vitoria 1729, 29040-780, Jucutuquara, Vitória/ES, Brazil
joaothomazlemos@gmail.com, pablorm@ifes.edu.br, regisbn@ifes.edu.br
[2]*Dept. of Electrical Engineering, Federal Institute of Espírito Santo*
andrieleninke@gmail.com, josemars@ifes.edu.br
[3]*Institute of Health and Biotechnology, Federal University of Amazonas*
Estrada do Aeroporto, 305, 69460-000, Urucu, Coari/AM, Brazil
herculeslmc@hotmail.com

Abstract. With the emergence of the Covid-19 pandemic, sanitary barriers that use infrared thermography have become more relevant as a means of combating the spread of this type of disease, as it is a non-contact diagnosis method. A crucial factor when working with thermography is the emissivity of the analyzed surface, a base parameter that thermal imagers use to estimate the temperature. For human skin, researchers generally adopt the emissivity value of 0.98. However, this value considers only the condition of dry skin in its natural state. Therefore, it is necessary to estimate the emissivity of the skin in other conditions, such as sweating skin, which are common in passersby of sanitary barriers. In this paper, the authors present an experimental procedure to obtain the forehead emissivity of volunteers by using the electric tape method and a developed a computer program algorithm based on Planck's Law of Thermal Radiation to enhance this method. Both approaches, the electrical tape method with and without the developed algorithm, were applied to thermographic images of thirty-six volunteers. Both methods obtained similar results, showing that it is possible to use the developed algorithm with the electrical tape method, enabling emissivity estimates to be more efficient.

Keywords: Skin Emissivity; Infrared Thermography; Temperature Measurement.

1 Introduction

Infrared thermography has been increasingly relevant in the health field, specifically, when used for detecting people in a feverish state in sanitary barriers, it allows for measuring body temperature without contact and in real-time [1]. In December 2019, SARS-CoV-2, the causative agent of COVID-19, was detected for the first time (Coronavirus Disease 2019) in China. In January 2020, the World Health Organization (WHO) declared the disease a global epidemic [2]. Thenceforth, several countries have adopted sanitary barriers based on infrared thermography. Since fever is one of the most common symptoms of this disease [3], one of the ways to combat its propagation is tracking of feverish people. Thus, this technique has gained prominence in the fight against the disease. The infrared radiation emitted by the inspected surface is the main parameter in metrological terms for temperature estimates by thermography, and its calculation uses the emissivity of this surface as the main parameter [4]. Literature indicates that the emissivity value of human skin varies between 0.95 and 0.99 [5]–[8]. In sanitary barriers, generally, a default value of 0.98 is adopted. However, this default value only corresponds to the state of natural and dry skin [8].

In 2009, Nishiura and Kamiya [9] performed a case study to verify the accuracy of the diagnosis of febrile states using infrared thermography. They concluded that the specificity and sensitivity for fever detection ranged from 50.8 to 70.4% and 63 .6% to 81.7%, respectively. The low reliability of the method may be because in the sanitary barriers, conditions that affect the emissivity, such as sweating of the skin or skin with some lotion, are not being considered. Another factor associated with low reliability in the diagnosis by infrared thermography is

the area of the body analyzed (ROI - region of interest), since different parts of the surface of the human body have different temperatures, despite the central temperature being practically constant. According to [10], the face is the most suitable place for temperature measurement by thermography, as it represents the body's internal temperature with high fidelity, unlike other regions such as the wrist. In sanitary barriers, the forehead should be the ROI to be analyzed by thermal imagers, as it is the place most likely to be free of facial accessories.

The thermal imager's embedded software, FLIR Tools 4.1, allows the manual insertion of the emissivity value of the surface to be analyzed. So that when reading the infrared radiation of this surface, it indicates the proper temperature. The initial procedure is to enter the emissivity of the tape used as a reference and take note of the tape and surface temperatures. The tape temperature reading corresponds to both surface and electrical tape temperatures. The apparent surface temperature is not read correctly since the emissivity corresponds only to the tape. Next, it is necessary to set the emissivity to the value at which the surface apparent temperature is equal to the initial temperature of the tape. Usually, this emissivity is defined by trial and error. Once the electrical tape and the surface are in thermal equilibrium, the new emissivity can be considered the correct emissivity of the analyzed surface [6], [11].

The present work proposes to estimate the emissivity of human skin as a function of conditions such as dry skin, skin with facial lotion, and sweat skin. For this, we performed an experiment organized in steps, considering the acquisition of the forehead thermographic images of volunteers in three different skin states (dry, sweaty, and with lotion) and analyzing these images in the software provided by the thermal imager manufacturer. The first step was to estimate the emissivity using the electrical tape method, a technique widely used to find a surface emissivity being the tape emissivity previously known [11]. In this method, the electrical tape is glued to the surface to be inspected (forehead), waiting until both are in thermal equilibrium. Then, they capture the image with the thermal imager. Finally, we analyze the temperatures using the embedded software. Here it is possible to obtain and evaluate the reading of the apparent temperature of the tape and the surface. As one of the steps of this method involves the manual definition by trial and error of the emissivity parameter in the software, this work also proposes the development of a computational algorithm in the Python programming language that will have the function of automating this step.

2 Methodology

2.1 Physical-mathematical fundamentals

For the trial and error step to be eliminated from methods to estimate the emissivity, such as the tape method, there is a need to develop a computational algorithm that, upon receiving the temperature and emissivity information of the object used as a reference, and the apparent surface temperature, estimate the emissivity of that surface automatically. Building this software required a review of Planck's Radiation Law and its relationship with infrared thermography. Planck's Law of Thermal Radiation, which is used to find the power of radiation emitted by a black body at a temperature T and wavelength λ, is described in eq. (1) [11].

$$M(T,\lambda) = \frac{2\pi hc^2}{\left(e^{\frac{hc}{\lambda k T}}-1\right)\lambda^5} \tag{1}$$

where $M(T,\lambda)$ is the radiation power for a defined wavelength and temperature, given in $J.s^{-1}$, h is Planck's constant, $6{,}62606957\ x\ 10^{-34} J.s$; c is the speed of light in vacuum, $2{,}9979246\ x\ 108\ m.s^{-1}$, and k is Boltzmann constant, $1{,}3806488\ x\ 10^{-23}\ J.K^{-1}$.

The total radiation energy of a surface J, inspected by the thermal imager, can be described as the energy of the surface itself E added to the energy that arrives by external means from the environment, reflected in the inspected surface G [11], as can be seen in eq. (2). The variables J, E and G defined here are cases of $M(T,\lambda)$.

$$J = \varepsilon E + \rho G \tag{2}$$

where ε is the surface emissivity, which determines the fraction of surface radiation that is emitted to the medium, and ρ is the reflectivity, which determines the portion of energy that reaches the inspected surface from the environment and is reflected to the environment [11]. However, ρ is complementary to ε, so eq. (1) can be written in the form of eq. (3).

$$J = \varepsilon E + (1-\varepsilon)G. \tag{3}$$

2.2 Proposed method

Considering that the method is carried out in a controlled environment, both the tape and the forehead are under the influence of the same radiation emitted by the environment (G), which can be calculated from the environment temperature. In addition, the thermal imager manufacturer previously establishes the wavelength range supported by equipment, ranged by $\lambda_1 = 8.5\ \mu m$ to $\lambda_2 = 13\ \mu m$. Initially, when entering in the software the emissivity value of the tape, ε_1, the temperature of the tape T_1 will be indicated, and with that, the value of the energy of the tape E_1. Considering the forehead energy as E_2, as the temperature of the forehead and the tape are equal, it can be said that $E_1 = E_2$. The radiation power that reaches the thermal imager from the forehead is given by J_2. For the emissivity parameter equal to ε_1, the apparent forehead temperature T_{aux} is not correct since ε_1 is the electrical tape emissivity, and ε_2 is the emissivity of the forehead. The energy E_{aux} obtained from T_{aux} is used in eq. (4) to calculate the forehead radiation power J_2. In order to calculate the radiation powers given by E_{aux}, E_1 and G, it is necessary to integrate eq. (1) with lower limit λ_1 and upper limit λ_2, using their corresponding temperatures.

$$J_2 = \varepsilon_1 E_{aux} + (1 - \varepsilon_1)G. \tag{4}$$

When entering the emissivity ε_2 corresponding to the forehead temperature value T_2, indicated by the thermal imager, that is equal to the tape temperature value T_1, we would then have the tape energy E_1 from T_1. Eq. (5) shows the calculation of the forehead radiation power J_2 received by the thermal imager from these new parameters.

$$J_2 = \varepsilon_2 E_1 + (1 - \varepsilon_2)G. \tag{5}$$

Thus, to calculate the forehead emissivity, we must equate eq. (4) and eq. (5), in order to obtain eq. (6).

$$\varepsilon_2 = \frac{\varepsilon_1(E_{aux} - G)}{E_1 - G}. \tag{6}$$

From the eq. (6), a computational algorithm to automate the step of obtaining the forehead emissivity was developed. To implement the algorithm, the version 3.10 of Python was used, in the integrated development environment (IDE) PyCharm 2022. The machine used in the experiments is equipped with Intel Core i5 2,6 GHz processor, 8 Gb RAM and Windows OS.

The input parameters were the temperatures of the environment, electrical tape, the apparent temperature of the forehead, in Celsius degrees, and the value of the tape emissivity. The algorithm first initializes the constants needed and transforms input temperatures to Kelvin units, then, integrates the E_{aux}, E_1 and G using their respective inputs in association with the fixed values of $\lambda_1 = 8.5\ \mu m$ to $\lambda_2 = 13\ \mu m$, with the *quad* function. At last, it computes and returns the desired emissivity. The workflow can be visualized in Fig. 1.

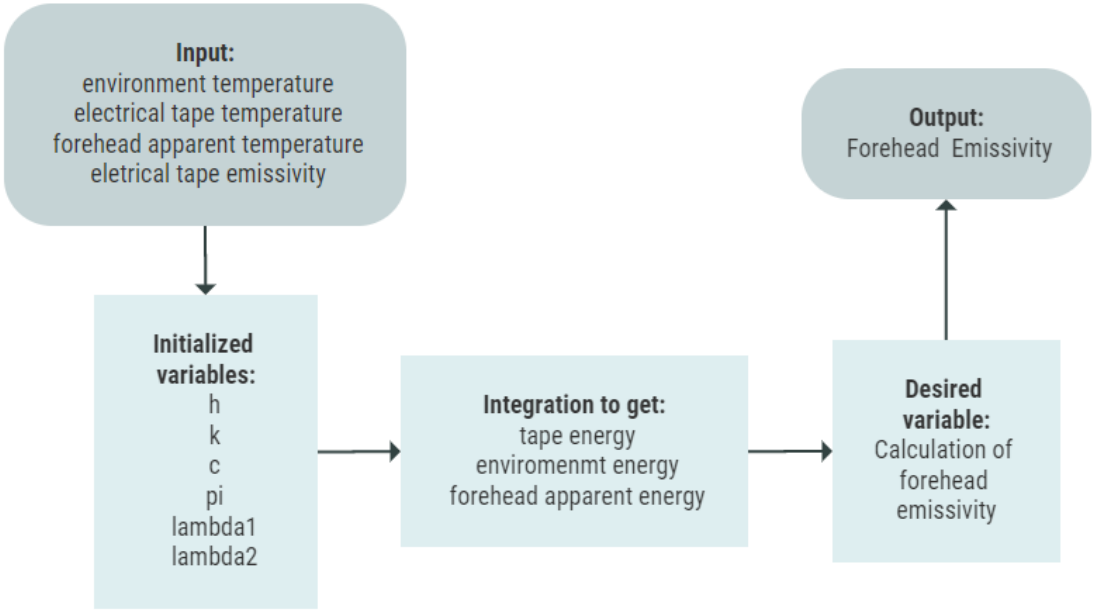

Figure 1. Algorithm workflow

To do the numerical integration, Quad function from the python library SciPy 1.9.0 was used [12]. This function uses numerical quadrature technique from Fortran library QUADPACK to compute finite integrals [13]. Quad evaluates the accuracy of integration based on whether the difference between computed result and the numerical approximation is greater than the tolerance error or not, as it is used for the stop criteria [12].

As the function parameters have finite bounds, no break points like singularities and no weight function were needed, and it uses the QAGS routine from QUADPACK. For tolerance and stop criteria, the function default values integration absolute error tolerance of $1.49e^{-8}$ and an upper limit of 50 subintervals for the adaptive algorithm between λ_1 and λ_2 [14] were defined in order to get reliable results, because in this way, the error dimensionality is much lower than the integration computed.

For validation of the emissivity's values calculated and generated by the developed algorithm, the metric roots mean squared error ($RMSE$) was used [15], given by eq. (7). This metric was chosen because it is regularly employed in model evaluation studies and it calculates the average error of the analyzed samples [16], which are values that can be easily interpreted as they are in the same dimensionality of the analyzed numbers. The sample size *n* was 12 for each skin condition, which was enough [16] for the $RMSE$ results to be reliable.

$$RMSE = \sqrt{\frac{\sum_{i=1}^{n}(\hat{y}_i - y_i)^2}{n-1}} \tag{7}$$

where $\hat{y}$ is the emissivity estimate generated by the proposed algorithm, y is the emissivity value given by the software with the "trial and error" technique, adopted here as the agreed true value, and n is the number of measurements.

3 Results and Discussion

The experiment proposal had been to determine the emissivities of the human body considering three skin states - dry skin, skin with lotion, and sweat skin, in a controlled environment, whose temperature was approximately 23 °C. In addition, the emissivities would be obtained through the "try and error" method and by the developed algorithm and compared among them. After twelve measurements for each skin state, sufficient quantity to apply the RMSE metric [15], the results indicated a significant difference between the emissivity of dry skin and the other two considered skin states. According to [17], the 3M SUPER 33 electrical tape has an emissivity value of 0.96. The results present the precision of two decimal places due to the instrument resolution. Besides, the thermal imager works on a wavelength range from 8.5 µm to 13 µm. Tables 1, 2, and 3, show the emissivity values, and the data used as input of the algorithm, like the ambient temperature, the electrical tape temperature, and the auxiliary temperature from the forehead.

Table 1 shows the comparison between the emissivities obtained by the "try and error" and by the proposed algorithm. The calculated RMSE for dry skin measurements was 0.003. This indicates that the error is less than the resolution of the software's input data, i.e., two significant figures. The same occurs for skin with lotion and sweat skin, whose RMSE values were 0.005 and 0.004, respectively. Thus, it is concluded these values were metrologically similar.

Table 1. Measures for dry skin condition

Measure	Room Temperature (°C)	Tape Temperature (°C)	Apparent Forehead Temperature (°C)	FLIR Emissivity	Algorithm Emissivity
1	26.2	35.1	35.0	0.95	0.95
2	26.1	35.2	34.9	0.93	0.93
3	26.1	35.7	35.5	0.93	0.94
4	26.1	35.7	35.6	0.95	0.95
5	26.1	35.4	35.5	0.97	0.97
6	27.1	35.9	35.8	0.95	0.95
7	27.1	34.4	34.1	0.92	0.92
8	26.3	35.2	35.3	0.97	0.97

9	26.3	34.9	34.7	0.94	0.94
10	23.9	34.7	34.6	0.95	0.95
11	23.7	34.2	34.1	0.95	0.95
12	24.5	35.0	35.1	0.97	0.97

Table 2. Measures for skin condition with lotion

Measure	Room Temperature (°C)	Tape Temperature (°C)	Apparent Forehead Temperature (°C)	FLIR Emissivity	Algorithm Emissivity
1	26.1	34.8	34.1	0.88	0.88
2	26.1	35.5	35.1	0.91	0.92
3	26.1	35.5	33.9	0.79	0.79
4	26.1	35.3	34.5	0.87	0.87
5	26.1	34.5	34.0	0.90	0.90
6	26.4	34.4	33.1	0.80	0.80
7	26.4	33.9	33.2	0.87	0.87
8	26.4	35.1	33.7	0.80	0.80
9	23.9	34.0	32.6	0.82	0.82
10	23.6	33.5	31.8	0.79	0.79
11	24.2	35.2	33.5	0.81	0.80
12	24.0	33.4	32.4	0.86	0.85

Table 3. Measurements for skin condition with sweat

Measure	Room Temperature (°C)	Tape Temperature (°C)	Apparent Forehead Temperature (°C)	FLIR Emissivity	Algorithm Emissivity
1	25.9	35.9	34.0	0.77	0.77
2	25.9	35.5	34.0	0.81	0.81
3	25.9	35.4	34.6	0.87	0.87
4	25.9	35.9	33.8	0.75	0.75
5	26.4	35.4	34.1	0.82	0.82
6	26.4	35.2	34.0	0.82	0.82
7	26.4	35.4	33.2	0.72	0.72
8	23.8	36.3	34.6	0.82	0.82
9	23.8	32.2	29.9	0.69	0.70
10	23.5	34.5	33.2	0.84	0.84
11	23.9	35.2	33.8	0.84	0.83
12	27.0	36.1	35.2	0.86	0.86

Table 4. Average Emissivity and Standard Deviation

Skin State	(FLIR) Average Emissivity	(FLIR) Standard Deviation	(Algorithm) Average Emissivity	(Algorithm) Standard Deviation
Dry	0.95	0.02	0.95	0.02

Lotion	0.84	0.04	0.84	0.05
Sweat	0.80	0.06	0.80	0.05

Aiming to highlight the difference between the emissivity for dry skin and the others, table 4 presents the average emissivities and standard deviations corresponding to the three skin states obtained through two approaches, electrical tape and algorithm.

A variation in emissivity was obtained for different skin conditions, especially between dry skin and other skin states. For example, the average emissivity on skin with lotion is about 11.6% lower than on dry skin. This difference is enough to affect the screening of people, since the temperature threshold for fever is very close to standard body temperature. Therefore, small increases or decreases in the measured temperature can misclassify the individual as febrile or non-febrile. In sweaty skin, this difference is more relevant and reaches 15.8%, which can compromise the accuracy. The use of adequate emissivity values for temperature measurement in sanitary barriers is shown to be an indispensable feature to achieve better results in the screening of febrile people.

When using the algorithm, we obtain an emissivity value instantly, which is an advantage over trying to guess the emissivity, a step that can take up to a minute for each sample.

4 Conclusions

The achieved results by the developed algorithm were practically the same as those obtained by try and error. Although the proposed method uses a surface with known emissivity, this drawback does not reduce the benefits of a higher degree of automation in estimating the skin emissivity during temperature measurement. On the other hand, the tape method is not practical to be applied in real time during the screening process of febrile people, since it is based on trial and error. Thus, the developed algorithm can be used to make the tape method more efficient, since it speeds up the step of determining the emissivity. Besides, it allows applying the method using other materials of known emissivity as reference, as well as, working with equipment that operates on different wavelengths.

Estimating the real-time skin emissivity value during screening of febrile people is not as important as knowing the skin condition. Once the mean emissivity has been determined for each skin condition a more accurate value can be used in estimating the temperature. For this, it is necessary to identify the condition in which the skin is. Thus, automatic detection of the skin condition by images is presented as a proposal for future works.

Acknowledgements. This work was supported by FAPES (Espírito Santo Research and Innovation Support Foundation), grant numbers 03/2020 (Induced Demand Assessment–COVID-19 Project), and 04/2021 (Research Support); IFES (Federal Institute of Espírito Santo), grant numbers 10/2021 (Institutional Support Program for Stricto Sensu Graduate Studies – PROPÓS), and 08/2022 (Institutional Program for Scientific Diffusion – PRODIF); and CNPq (National Council for Scientific and Technological Development), grant number 02/2020 (Productivity Scholarship in Technological Development and Innovative Extension - DT).

Authorship statement. The authors hereby confirm that they are the sole liable persons responsible for the authorship of this work, and that all material that has been herein included as part of the present paper is either the property (and authorship) of the authors, or has the permission of the owners to be included here.

References

[1] D. S. Haddad, M. L. Brioschi, M. G. Baladi, and E. S. Arita, "A new evaluation of heat distribution on facial skin surface by infrared thermography," *Dentomaxillofacial Radiol.*, vol. 45, no. 4, pp. 1–10, 2016, doi: 10.1259/dmfr.20150264.

[2] R. M. Lana *et al.*, "The novel coronavirus (SARS-CoV-2) emergency and the role of timely and effective national health surveillance," *Cad. Saude Publica*, vol. 36, no. 3, 2020, doi: 10.1590/0102-311x00019620.

[3] A. Bassi, B. M. Henry, L. Pighi, L. Leone, and G. Lippi, "Evaluation of indoor hospital acclimatization of body temperature before COVID-19 fever screening," *J. Hosp. Infect.*, vol. 112, pp. 127–128, 2021, doi: 10.1016/j.jhin.2021.02.020.

[4] P. R. Muniz, R. de Araújo Kalid, S. P. N. Cani, and R. da Silva Magalhães, "Handy method to estimate uncertainty of temperature measurement by infrared thermography," *Opt. Eng.*, vol. 53, no. 7, p. 074101, 2014, doi: 10.1117/1.oe.53.7.074101.

[5] T. Togawa, "Non-contact skin emissivity: measurement from reflectance using step change in ambient radiation temperature," *Clin. Phys. Physiol. Meas.*, vol. 10, pp. 39--48, 1989, doi: 10.1088/0143-0815/10/1/004.

[6] M. Charlton *et al.*, "The effect of constitutive pigmentation on the measured emissivity of human skin," *PLoS ONE*, vol. 15, no. 11 November. 2020, doi: 10.1371/journal.pone.0241843.
[7] F. J. Sanchez-Marin, S. Calixto-Carrera, and C. Villaseñor-Mora, "Novel approach to assess the emissivity of the human skin," *J. Biomed. Opt.*, vol. 14, no. 2, p. 024006, 2009, doi: 10.1117/1.3086612.
[8] I. Fernández-Cuevas *et al.*, "Classification of factors influencing the use of infrared thermography in humans: A review," *Infrared Phys. Technol.*, vol. 71, pp. 28–55, 2015, doi: 10.1016/j.infrared.2015.02.007.
[9] H. Nishiura and K. Kamiya, "Fever screening during the influenza (H1N1-2009) pandemic at Narita International Airport, Japan," *BMC Infect. Dis.*, vol. 11, pp. 1–11, 2011, doi: 10.1186/1471-2334-11-111.
[10] F. D. S. Santos, P. R. Muniz, J. Simão, and J. Da Silva, "Comparative analysis of the use of pyrometers and thermal imagers in sanitary barriers for screening febrile people," *IEEE Int. Conf. Ind. Appl.*, vol. 14, 2021, doi: 10.1109/INDUSCON51756.2021.9529880.
[11] M. Vollmer and K. P. Möllmann, *Infrared thermal imaging: Fundamentals, research and applications*. Weinheim: WILEY-VCH Verlag GmbH & Co., 2010.
[12] P. Virtanen *et al.*, "{SciPy} 1.0: Fundamental Algorithms for Scientific Computing in Python," *Nat. Methods*, vol. 17, pp. 261–272, 2020, doi: 10.1038/s41592-019-0686-2.
[13] D. K. Robert Piessens, Elise deDoncker-Kapenga, Christian Ueberhuber, *QUADPACK: A Subroutine Package for Automatic*, 1st ed. New York.
[14] J. R. Rice, "A Metalgorithm for Adaptive Quadrature," *J. ACM*, vol. 22, no. 1, pp. 61–82, 1975, doi: 10.1145/321864.321870.
[15] A. G. Barnston, "Correspondence among the correlation, RMSE, and Meidke Foresast verification measures; Refinement of the Neidke Score," *Weather and Forecasting*, vol. 7, no. 4. pp. 699–709, 1992, doi: 10.1175/1520-0434(1992)007<0699:CATCRA>2.0.CO;2.
[16] T. Chai and R. R. Draxler, "Root mean square error (RMSE) or mean absolute error (MAE)? -Arguments against avoiding RMSE in the literature," *Geosci. Model Dev.*, vol. 7, no. 3, pp. 1247–1250, 2014, doi: 10.5194/gmd-7-1247-2014.
[17] FLIR Systems, "User's Manual FLIR Exx series," 2013. http://www.flir.com (accessed May 08, 2022).